Hindawi
Advances in Materials Science and Engineering
Volume 2022, Article ID 8579180, 13 pages
https://doi.org/10.1155/2022/8579180

Research Article

Hybrid RSA-ROA Scheduling Algorithm for Minimization of Power Loss and Improving the Renewable with Sustainable Energy Harvesting in Power System

Cuddapah Anitha,[1] **Virendra Swaroop Sangtani**,[2] **Ajay Kumar Bansal**,[3] **Mahaveerakannan R.**,[4] **R. Rajesh Sharma**,[5] **and Saravanan M. S.**[6]

[1]*Department of Computer Science and Systems Engineering, Sree Vidyaniketan Engineering College, Tirupati, Andhra Pradesh, India*
[2]*Department of Electrical Engineering, Swami Keshvanand Institute of Technology, Management & Gramothan, Jaipur, Rajasthan, India*
[3]*Department of Electrical Engineering, Central University of Haryana, Mahendergarh, Haryana, India*
[4]*Department of Computer Science and Engineering, Saveetha School of Engineering, Saveetha Institute of Medical and Technical Sciences, Chennai, Tamil Nadu, India*
[5]*Adama Science and Technology University, Adama-1888, Ethiopia*
[6]*Department of Artificial Intelligence, Saveetha School of Engineering, Saveetha Institute of Medical and Technical Sciences, Chennai, India*

Correspondence should be addressed to R. Rajesh Sharma; sharmaphd10@gmail.com

Received 21 June 2022; Accepted 16 July 2022; Published 16 August 2022

Academic Editor: Vijayananth Kavimani

Recently, it has been very common for wireless sensor networks (WSNs) to be used in several applications (surveillance, home automation, and vehicle tracking), as well as in environmental monitoring and wildlife tracking. A typical sensor node has a limited amount of battery life. To overcome this, one method is to use an energy harvesting device to recharge the batteries of sensor nodes. Energy reaping WSNs still lack intelligent strategies for intelligently using both energy organization and harvesting systems, though. To maximize the harvesting of renewable energy sources (RES) and minimize power scheme losses, this study provides an optimal generation scheduling strategy for a power scheme combined with distributed generation (DG) and sustainable energy storage systems (ESSs). The major goal of this work is to make it possible to use RES in a power system while still maintaining a profit. By using ESS management, we are able to get the most out of our renewable energy resources and maximize our harvesting potential. It is also possible to reduce operating losses in the power system by scheduling ESS and controlled generation at the optimal times. Near global optimal solutions are sought using a hybrid algorithm combining Reptile Search Algorithm and Remora Optimization Algorithm (RSA-ROA). The power system operational restrictions are taken into account when formulating and evaluating the optimization issue. It has been tested in a variety of circumstances to see if the proposed strategy is effective. The proposed model has 0.260 J of remaining energy, when the number of rounds is 5000, but the existing techniques have only 0.110 J and 0.045 J for the same number of rounds.

1. Introduction

WSNs are made up of a limited sum of low-cost and low-power sensors. Multiple tasks such as data sensing and simple computing can be performed by the network, as well as short-distance transmission and storage for temporary data [1, 2]. In addition to health monitoring, transportation tracking, environmental monitoring, and border surveillance, it is employed in various uses of Internet of Things [3]. Energy consumption in sensor networks is closely connected

to their longevity because of the battery's major role in supplying power. Sensor nodes in traditional sensor networks have been batteries with a finite capacity. Although the sensor nodes have a partial battery life, the normal application will have a limited battery life as well. It takes a long time to replace the batteries of sensor nodes and making the network sustainable is often a challenging task, because they are often located in remote locations. As a result, prolonging the life of a network is a difficult task when faced with energy restrictions [4].

Researchers have found a way around the restrictions of energy harvesting technologies by adopting this method. An energy collecting technology can be used to power nodes indefinitely. The network's energy consumption can be optimized for maximum efficiency. Increasing the sampling frequency or duty cycle of a sensor node, for example, or increasing the transmission power to reduce the energy harvesting device is more favourable. Renewable energy resources include the energy gathering system [5]. A resource's ability to be replenished over time by natural processes is what is meant by the term "ambient energy resources." Sensor nodes are powered by a variety of sources, including photovoltaics, wind turbines, heat pumps, and other mechanically driven devices such as batteries [6–8]. Photoelectric cells transform the solar radiation into electrical energy, which is then used in an outdoor system during the daytime rather than at night or in overcast conditions [9]. Wind energy is rehabilitated into power energy by turbines in the wind energy-based system. There are two ways to shift the turbines: horizontally and vertically. It also uses piezoelectric or electrostatic devices to turn heat into electricity, as well as TEGs to convert mechanical electricity. As a result of the unpredictable nature of energy collecting, managing energy supplies is a difficult endeavour. Wind and solar energy harvesting systems [10–13] use prediction as a well-known approach of managing renewable resources. In contrast, several contemporary WSNs that harvest energy lack a smart approach for judiciously utilizing the management and harvesting systems. Energy harvesting and battery replacement will be discussed in detail in the following paragraphs.

Battery Replacement. An efficient and successful operating system requires regular battery replacement. The central remote station constantly monitors the battery's condition. Maintenance personnel or a team may be dispatched to the remote location to replace a low-battery device. To avoid this problem, an additional battery or energy source should be added to the sensor node. This solution is either practical, cost-efficient, or flexible for effective and sustainable WSNs because of the high energy consumption of sensor nodes in dynamic operations.

Energy Harvesting in Sustainable Manner. Wind, solar, water, and other natural energy bases can all be used to generate electricity, as well as pressure, heat, and vibration. Low-power sensor nodes can now last an indefinite amount of time thanks to energy harvesting, which has to be done in a sustainable manner. Single-source energy harvesting is a superior option for long-term WSN sustainability. When adopting single-source energy harvesting, however, irregular and insufficient battery charging might have a negative impact on the system's stability [14–16].

With the hybrid technique of energy harvesting, it is possible to build and execute an enhanced WSN that can increase the lifespan data collection, actuation, and processing, and transmission is another option for a WSN that is effective, long-lasting, and sustainable. We therefore need clever solutions. Optimal generation scheduling is the focus of this research, which examines the best way to maximize renewable energy gathering while minimizing power losses. It is possible to identify the most important variables in RES-based electricity generation with DG and ESS using the proposed method. In practice, however, DG accommodations and dimensions cannot be modified due to producer capacity restrictions and economic benefit. DGs, in particular, are always situated in a certain location that cannot be controlled. Producers expect maximum DG outputs, while the power system's loss may rise because of this. The output power of DGs is therefore adjusted in a way that maximizes the gathering of renewable energy. Thus, enough power can be given to the loads, and extra power can be stored in ESS (Excessive Power Storage).

1.1. Organization of This Paper. The related study of the existing technique, which is related to our research study is mentioned in Section 2. The brief explanation of the proposed model is depicted in Section 3, and the validation analysis is presented in Section 4. Finally, the conclusion of the research work is given in Section 5.

2. Related Works

WSN generation depends on duty cycle, deployment type, and battery state-run of charge (SoC), according to Sharma [17]. Using ambient energy reaping to charge WSN node batteries, we provide a novel solution to the design challenge of low energy availability (LEA). Nevertheless, solar energy harvesting is fraught with difficulties, such as the inconsistency of the power supply and the inability to accurately estimate the sun's output, as well as problems related to temperature and the efficiency of the solar panels. The goal of this research is to extend the lifespan of WSNs by gathering solar energy. As shown by our simulations, the sensor network lifetime can be extended to an indefinite level, with an optimum duty cycle of 100%, up to 115.75 days. SEH-WSNs also saw an increase in network speed from 100 to 160 kilobits per second.

Liu [18] suggests a two-stage strategy for dealing with the dynamics of renewable energy. As part of the network preparation phase, we apply the primal cut approach to resolve an RO (two-stage) problem and build an efficient data gathering tree. With minimum overhead, we offer an algorithm that may maximize the sample rates of nodes based on the observed recharge rates. Network performance is maximized under renewable energy uncertainty by not having to reconfigure routing structure during operational

phase. The proposed strategy is shown to be successful and robust in coping with the fluctuation of renewable energy through numerical findings.

According to Gupta [19], there is an adaptive. Multisensing solutions based on network and node-level partnerships are proposed to boost energy efficiency. Instead of relying on cross-correlation among the recorded strictures at each node, the latter relies on nodes with active sensors (as determined by MS). MS-sensing SP's quality can be improved by using a retraining logic. Multisensor data fusion is presented to estimate all parameters across field nodes utilizing undersampled signals from the MS-CC active sensors.

A new protocol was proposed by Sah [20] for energy harvesting clusters (NEHCP). An algorithm called hierarchical clustering routing is used to implement the NEHCP, which employs solar EH. It is the cluster head's job to convey data collected from the sensor nodes back to the central station. The beginning phase, setup phase, and data transmission phase are all parts of the NEHCP algorithm. The EH-WSN feature gives better results in terms of network longevity because it is unique. The EH-WSNs' energy consumption is balanced and network efficiency is increased by the simulation element of this technology.

Two-port hybrid diodes and an adaptive supercapacitor buffer energy management technique are presented by Qi [21] to accomplish combined optimization. In the hybrid diode semiactive topology, the bidirectional DC/DC converter is replaced by a unidirectional DC/DC converter and two diodes instead of the current two. As a result, 15.5 percent less energy is lost, and the control system's cost, size, and complexity are all reduced. Adaptive supercapacitor buffer energy organization is also being developed using the novel architecture to reduce battery degradation. There is a minimum threefold increase in battery life compared to the current hybrid energy storage devices in simulations and experiments. Sensor nodes powered by sunlight for the first time have been made possible.

A wearable medical sensor device was designed by Mohsen for long-term medical use [22]. The acceleration of a human body can all be monitored in real time using this method. There are two sensors in this system: one for temperature and one for pulse oximetry. There is also a microprocessor and a Bluetooth low energy module in there. Batteries are required to power this sensor system, but they only last so long. An energy harvester that can power an array of wearable medical sensors is therefore being developed. The sensor system's lifespan can be extended thanks to this harvester, which generates enough energy to run the scheme. The suggested hybrid energy harvester is made up of two supercapacitors, a DC-DC boost converter and two flexible solar panels. For a total of 46 hours of operation, the sensor system was put to the test in active-sleep mode, where it consumed an average of 2.13 mW over a single hour. Finally, the findings of the experiments show that the medical sensor system may be monitored for an extended period of time.

A multihop data forwarding algorithm and decision-making model for the selection of data forwarding nodes were developed by Wu [23] for WSN powered by solar cells and batteries. The Pareto optimal collection of solutions can be found using the particle swarm optimization method. Energy supply models are developed after an investigation of solar energy acquisition aspects. An algorithm for forwarding information in response to changes in network energy consumption and delay has been demonstrated in simulated results.

3. Proposed System

In this section, first mathematical models for sustainable ESS and RES are explained.

3.1. Mathematical Ideal. Equations (1) and (2) describe the optimal generation preparation problem for maximizing energy gathering and reducing losses.

$$\text{Maximize } f_1 = \max\left(P_{\text{DG dispatch}}\right), \tag{1}$$

$$\text{Maximize } f_2 = \min\left(P_{\text{Lossline}}\right). \tag{2}$$

There are two sets of proposed goal functions: f_1 and f_2. The power system's P (DG dispatch) harvests renewable energy. In a transmission line, P (Loss line) represents the amount of power lost (MW).

3.1.1. Renewable Energy Harvesting Model. It is a fact of life that DGs are continuously run at their supreme rated power production. This could lead to unfavourable conditions for the power system, such as increased power losses. On the other hand, DG power cannot be directly controlled by the utilities. Renewable energy harvesting includes two components: DG dispatch of power and storage of power, which is the amount of power that can be stored between P (DG dispatch) and the maximum power that can be generated. ESS will store the extra power. The following is the function for gathering renewable energy sources:

$$P_{DG\,\text{dispatch}} = P_{DG\,\text{dispatch}} - P_{\text{storage}}. \tag{3}$$

Excess power is stored in ESS, where it is closely linked to power loss. These losses can be broken down into battery and converter losses, respectively [24], for the electric energy storage system (ESS). The following formula can be used to compute the ESS's loss:

$$\begin{aligned} P_{\text{LossESS}} &= P_{\text{Lossbatter}} + P_{\text{Lossconverter}}, \\ P_{\text{Lossbatter}} &= I_{\text{battery}}^2 \times R_{\text{battery}}, \\ P_{\text{Lossconverter}} &= P_{sb} + \left(k\% \times P_{\text{storage}}\right), \end{aligned} \tag{4}$$

where the battery and converter losses are denoted by $P_{\text{Lossbatter}}$ and $P_{\text{Lossconverter}}$, respectively. The internal resistance of the battery is R_{battery}. Power storage (P_{storage}) determines I_{battery} charging current. Standby power loss due to components is known as P_{sb} (continuous standby loss). Losses in semiconductors and filters account for k percent of the total.

This research, on the other hand, examines the direct link of the highest amount of renewable energy gathering. As a result, ESS loss is treated as if it were a property of P_{storage} rather than I_{batter}y. As shown in (3), P_{storage} has a considerable impact on ESS's power loss. Therefore, the ESS losses can be expected to be stowed power and ESS as follows:

$$\begin{aligned} P_{\text{storage}} &= P_{DG\,\text{output}} - P_{DG\,\text{dispatch}}, \\ P_{\text{LossESS}} &= (1-\eta)P_{\text{storage}}. \end{aligned} \tag{5}$$

3.1.2. Power Loss in Line Ideal. The generalised power flow is used in this study to determine the power losses in the power system's line. When analyzing the steady state of a real, the power flow equation can be expressed as follows [25]:

$$\begin{aligned} &S_i = P_i + jQ_i, \\ &P_i = \sum k = 1n|V_i||V_k||Y_{ik}|\cos(\theta_i - \theta_k - \alpha_{ik}), \quad i = 1, 2, \ldots, n, \\ &Q_i = \sum k = 1n|V_i||V_k||Y_{ik}|\sin(\theta_i - \theta_k - \alpha_{ik}), \quad i = 1, 2, \ldots, n. \end{aligned} \tag{6}$$

Net apparent power injections to bus I are represented by Si, P^i, and Q^i, respectively. Number of buses in the system is n. The magnitudes of the voltages on buses I and k are V^i and V^k, respectively. Both I and k refer to the voltage angles at the two buses in question. The difference in admission between buses I and k is measured by Y^{ik}. When two buses are in phase with one another, they are called "ik" and "k."

This work only covers the active component power losses in lines due to a branch conductance (g_{ik}) among buses I and k, which can be expressed as follows:

$$P_{\text{Lossline}_{ik}} = g_{ik}\left[V_i^2 + V_k^2 - 2V_iV_k\cos(\theta_i - \theta_k)\right]. \tag{7}$$

3.2. Objective Function Formulation. Achieving maximum energy means maximizing the DG's power output or decreasing the amount of excess energy that can represent the least amount of power loss in the ESS, as discussed in Sections 3.1.1 and 3.1.2. The proposed method's objective function is the product of (1) and (2). As a result, the following may be said about it:

$$\text{Min}\, P_{\text{Loss}}^{\text{Total}} = \sum_{i=1}^{Nl} P_{\text{Lossline},i} + \sum_{j=1}^{\text{Nst}} P_{\text{LossESS},j}. \tag{8}$$

Loss line i is defined as the power loss, and loss line j as the ESS loss. To put it another way, Nl and Nst represent the total sum of energy transmission lines and storage facilities.

3.3. Operational Constraints

3.3.1. Power Flow Constraint. When power is transmitted between any two buses I and j, where each bus is represented by a row and a column in Tables 1 and 2. An illustration of a power flow restriction is the following:

$$I_{i-j} \le I_{i-j}^{\max}, \tag{9}$$

Table 1: Details of IEEE 14-bus standard test scheme.

Type	Cap. (MW)	Bus
Renewable DG unit 1	100	12
Conventional gen. unit 2	600	2
Renewable DG unit 2	100	10
Conventional gen. unit 1	750	1
Conventional gen. unit 3	400	3
ESS unit 1		12
ESS unit 2		10
ESS unit 3		9

Table 2: Details of IEEE 30-bus test system.

Type	Cap. (MW)	Bus
Conventional gen. 1	200	1
Conventional gen. 2	150	2
Conventional gen. 3	150	5
Renewable DG 1	50	5
Conventional gen. 5	50	11
Conventional gen. 6	50	13
Renewable DG 3	50	9
ESS unit 1		5
ESS unit 2		3
ESS unit 3		9

where $I_{(i-j)}$ is the present line among buses$I$ and j, as shown in the figure. The line between buses I and j has a maximum current capacity of $I_{i-j}^{\max}$.

3.3.2. Generator Constraints. The system's generators must be run within the bus voltage's rated active and reactive power restrictions. The voltage must also fall within the acceptable ranges of maximum and minimum. The following are possible generator constraints:

$$\begin{aligned} P_N^{\min} \le P_N \le P_N^{\max}, \\ Q_N^{\min} \le Q_N \le Q_N^{\max}, \\ V_N^{\min} \le V_N \le V_N^{\max}. \end{aligned} \tag{10}$$

Generator bus N injects power (PN) both actively and reactively. Generator N's maximum active and reactive powers are referred to as PN max an d QN max. PN min an d QN min are generator N's minimal active and reactive powers. The voltage on the bus at which a generator is attached (bus N) is known as V_N. Voltages min are the generator bus's maximum and minimum operational voltages, respectively.

3.3.3. Renewable Distributed Generation Restraint. Only the maximum power output from the renewable DG source is taken into account. Here are some examples of how you can set a restriction:

$$0 \le P_{DG,N} \le P_{DG,N}^{\max}. \tag{11}$$

The active power transfer from DG to bus N is denoted by $P_{DG,N}$. DGs at bus N have a maximum active power of $P_{DG,N}^{\max}$.

3.3.4. Load Constraints. Distribute general load across system while maintaining voltage limitations as seen in (12). A voltage deviation (VD) limit must also be adhered to when operating the load. Difference in voltage between the maximum and minimum voltage limitations is referred to as *VD*. We can write *VD* down as follows:

$$\begin{aligned} &V_N^{\min} \le V_N \le V_N^{\max}, \quad N = 1, \ldots, n \text{ bus no,} \\ &VD_i = V_i^{\max} - V_i^{\min}, \quad i = 1, \ldots\ldots, m \text{ scenarios no.} \end{aligned} \tag{12}$$

Maximum and minimum bus voltage limitations are $V_N^{\max}$ and $V_N^{\min}$, respectively. Maximum and lowest system voltages for scenario I are $V_i^{\max}$ and $V_i^{\min}$, respectively.

3.4. Proposed Model: Background. For minimizing the power loss and maximizing the renewable energy harvesting as presented in Sections 3.1 to 3.3, the optimal solutions are explored by applying the hybrid RSA-ROA. With regard to this hybrid algorithm, an entirely new transition mechanism has been proposed, and its primary technique has been described.

3.4.1. Reptile Search Algorithm (RSA). Here, we will discuss the Reptile Search Algorithm (RSA). Reptile Search Algorithm (RSA) is based on the natural behaviour of crocodiles in the wild, including their encircling mechanics, hunting tactics, and social interactions [26].

Encircling Phase. This section introduces the RSA's exploratory activity (encircling). Crocodiles have two distinct ways of encircling prey: high-walking and belly-walking.

Iteration number is divided into four equal parts, and the total sum of iterations is also divided into four equal parts. Based on these scenarios, RSA alternates between exploration and exploitation search stages. Two key search algorithms are used to uncover better answers in the RSA exploration mechanisms, which examine search regions and approaches.

During this step of the search, only one criterion must be met. High-walking and belly-walking search methods are carried out according to $tT/4$ an d $t2\,T/4$ and $t > T/4$, respectively. The following equation shows how the position is updated:

$$x_{(i,j)}(t+1) = \begin{cases} \text{Best}_j(t) \times \eta_{(i,j)}(t) \times \beta - R_{(i,j)}(t) \times \text{rand}, & t \le \dfrac{T}{4}, \\ \text{Best}_j(t) \times x_{(r_1,j)} \times ES(t) \times \text{rand}, & t \le 2\dfrac{T}{4} \text{ and } t > \dfrac{T}{4}. \end{cases} \tag{13}$$

Equation (14) yields the hunting parameter $\eta_{(i,j)}$. No matter what, b will always be equal to 0.01. Equation (15) determines the reduction function $R_{(i,j)}$. There are four random numbers in this problem: r_1, r_2, $x(i, j)$, and N. The sense of evolution equation (16) gives us the probability parameter $ES(t)$.

$$\eta_{(i,j)} = \text{Best}_j(t) \times P_{(i,j),}, \tag{14}$$

$$R_{(i,j)} = \frac{\text{Best}_j(t) - x_{(r_2,j)}}{\text{Best}_j(t) + \varepsilon}, \tag{15}$$

$$ES(t) = 2 \times r_3 \times \left(1 - \frac{1}{T}\right). \tag{16}$$

It is an integer with the value. The following equation determines the difference parameter $P_{(i,j),}$:

$$P_{(i,j),} = \alpha + \frac{x_{(i,j)} - M(x_i)}{\text{Best}_j(t) \times \left(UB_{(j)} - LB_{(j)}\right) + \varepsilon'}. \tag{17}$$

In (18), $M(x_i)$ indicates the average position. These are the highest and lower limits, respectively, where it has a value of 0.1.

$$M(x_i) = \frac{1}{n} \sum_{j=1}^{n} x_{(i,j),} \tag{18}$$

Hunting Phase. This section discusses RSA's predatory tendencies. Crocodiles hunt in two ways, depending on their hunting habits: coordination and teamwork.

$t \le T$and t 3 $T/4$ are used for hunting coordination in this phase; if $t\,T$ and t 3 $T/4$ are used, then the hunting cooperation is accomplished. Equation (19) depicts the position-updating procedures:

$$x_{(i,j)}(t+1) = \begin{cases} \text{Best}_j(t) \times P_{(i,j)}(t) \times \text{rand}, & t \le 3\dfrac{T}{4} \text{ and } t > 2\dfrac{T}{4}, \\ \text{Best}_j(4) - \eta_{(i,j)}(t) \times \varepsilon - R_{(i,j)}(t) \times \text{rand}, & t \le T \text{ and } t > 3\dfrac{T}{4}, \end{cases} \tag{19}$$

where the best solution is found, and the hunting parameter $\eta_{(i,j)}$ is defined by equation (14). According to equation (17), $P_{(i,j),}$ is the difference parameter. Equation (15) defines reduction function $R_{(i,j)}$.

3.4.2. Remora Optimization Algorithm (ROA). The detailed explanation of ROA [27] is given in the upcoming section.

Free Travel. SFO Strategy (20) provided the procedure's elite idea, which was used to model this algorithm's location update.

$$R_i^{t+1} = R_{\text{best}}^t - \left(\text{rand} \times \left(\frac{\left(R_{\text{best}}^t - R_{\text{ran d}}^t\right)}{2} \right) - R_{\text{rand}}^t \right), \tag{20}$$

where R_{rand}^t is a random location.

Experience Attack

The tuyu must take little steps around the host on a regular basis in order to regulate whether or not it is essential to replace the host. The following is the formula for simulating the aforementioned principles:

$$R_{\text{att}} = R_i^t - \left(R_i^t - R_{\text{pre}}\right) \times \text{rand}n. \tag{21}$$

In this example, R_{pre} is where the previous iteration left off, and R_{att} represents a tentative stride in that direction.

Because of this step's fitness evaluation, the current solution $f(R_i^t)$ and the attempted solution $f(R_{\text{att}})$ are described. If, for example, the proposed solution's fitness function value is lower than the fitness function value, then the proposed solution should be rejected.

$$f\left(R_i^t\right) > f\left(R_{\text{att}}\right). \tag{22}$$

This section shows how Remora uses a different technique for local optima than does the rest of Remora.

$$f\left(R_i^t\right) < f\left(R_{\text{att}}\right). \tag{23}$$

Eat Thoughtfully

WOA Strategy

As shown in the equations below, the location update formulation of Remora attached to the whale was reconstructed using the original WOA method:

$$\begin{aligned} R_{i+1} &= D \times e^{\alpha} \times \cos(2\pi\alpha) + R_i, \\ \alpha &= \text{rand} \times (a-1) + 1, \\ a &= -\left(1 + \frac{t}{T}\right), \\ D &= \left|R_{\text{best}} - R_i\right|. \end{aligned} \tag{24}$$

When a Remora is attached to a whale, their locations may be viewed as the same in the broader solution space. It is a number that decreases exponentially in the range of [−2, −1] and is chosen at random from the range of [−1, 1].

Host Feeding

Host feeding is a subcategory of the exploitation method. Host location can be reduced to the optimal solution at this stage. As a mathematical concept, travelling on or around the host is an appropriate way to describe incremental stages:

$$\begin{aligned} R_i^t &= R_i^t + A, \\ A &= B \times \left(R_i^t - C \times R_{\text{best}}\right), \\ B &= 2 \times V \times \text{rand} - V, \\ V &= 2 \times \left(1 - \frac{t}{T}\right). \end{aligned} \tag{25}$$

In this case, A was used to indicate a very small movement connected to the physical space occupied by the host and remora. To tell the difference between the host and Remora, researchers used a Remora factor (C). If the host has a volume of one, the Remora's volume is equal to one hundredth of that volume.

3.4.3. The Proposed Hybrid Method. RSA and ROA with a novel transition mechanism are combined in this part to present the primary technique for the proposed hybrid search algorithm.

In the suggested HRSA, a new mean transition mechanism and two major search strategies can alleviate many issues. Early global and local search algorithms are shortcomings of classical RSA. Nevertheless, it remains the most popular way to conduct a search. As a result, local search and early convergence are avoided by using the ROA search technique. ROA is used as a search engine as well as to

improve the efficiency of search. As a result, new ideas from other places can effectively broaden the search space. More robust approaches to achieving better results are inspired by these proposals for the proposed model.

Initialization Phase. Starting with a collection of candidates (X) generated stochastically, the optimization process in RSA commences. Nearly optimum solutions are found in each iteration.

$$X = \begin{bmatrix} x_{1,1} & \cdots & x_{1,j} & x_{1,n-1} & x_{1,n} \\ x_{2,1} & \cdots & x_{2,j} & \cdots & x_{2,n} \\ \cdots & \cdots & x_{i,j} & \cdots & \cdots \\ \vdots & \vdots & \vdots & \vdots & \vdots \\ x_{N-1,1} & \cdots & x_{N-1,j} & \cdots & x_{N-1,n} \\ x_{N,1} & \cdots & x_{N,j} & x_{N,n-1} & x_{N,n} \end{bmatrix}, \quad (26)$$

where $x(i, j)$ is the jth location of the ith solution and N is the total sum of solutions and n is the size of the dimension derived from the following equation:

$$x_{ij} = \text{rand} \times (UB - LB) + LB, \quad j = 1, 2, \ldots, n, \quad (27)$$

where rand is a random and LB and UB signify the bound, correspondingly. The flow chart of the proposed model is given in Figure 1.

The Projected Mean Transition Mechanism (MTM). At the beginning of this section, Algorithm 1 provides an explanation of the mean transition mechanism (MTM). Controlling the search and switching between the RSA and the MT are both possible with this method. It takes a lot of skill to move from one search method to the next. It calls for an efficient method of changing the update operations across multiple techniques. When the fitness does not improve after five iterations, the basic idea behind the MTM is to regulate the search approaches (I). The number of repetitions decreases if there are no benefits to be had through testing.

While the fitness function value and C serve as a counter in Algorithm 1, the TM variable can be switched from 0 to 1 to alter the search process between RSA and MT. There are a maximum number of repeats I that should be altered if no improvements are seen.

4. Simulation Results and Discussion

4.1. Test Systems Description. The projected technique is put to test using IEEE 14-bus and 30-bus test schemes, side by side. According to the test systems, the generation units include generation and renewable DG units. Each renewable DG unit has an ESS installed to collect any extra power generated. In each site, the DG power output is a combination of the electricity energy available from the DG dispatch and the extra power stored in the ESS unit, which has different standards. Tables 1 and 2 present the component data for the 14-bus and 30-bus test systems, respectively. The efficiency of ESS is assumed to be 90% in all deployed locations for the purpose of calculating ESS losses.

The proposed WSN is being tested using MATLAB 2014 software. Table 3 shows the results of two distinct simulations. Table 4 has further information. During the simulations, we measure efficiency, the sum of active nodes, the network's average energy consumption, the First Node Dies (FND), the loss of 10% and 20% of nodes, and the number of packages transferred.

Depending on their level of sophistication, energy collecting nodes can be classified as basic or sophisticated. During different simulations, the percentages of normal and advanced nodes in the network are 80 percent and 20 percent, respectively. Nodes in the advanced stage have three times the energy of those in the standard stage. We ran a number of simulations, and the mean results are shown here. Table 3 shows the simulations scenario of the proposed model; here we used 100 and 200 nodes for simulation, as well as the areas of $500 \times 500\,\text{m}^2$ and $300 \times 300\,\text{m}^2$, respectively.

Table 4 shows the different parameters used in simulation, which are used in the proposed model.

In the FND analysis, when the time is 44.4 s, the hybrid RSA-ROA method has 40439 packets for 100 noded. But the single algorithm such as RSA and ROA has only 2410 packets and 3986 packets for the same number of nodes (100). When the number of nodes is 80, the hybrid model has 125268 packets, where the single models have only 5213 and 6535 packets for the analysis of PND. Next, Table 5 presents the summary for FND and PND for network 2.

From the comparative analysis in Table 6, it is shown that different types of PND, 200, 180 and 160, are used. In the FND analysis on 200 nodes, when the time is 361.2 s, the hybrid RSA-ROA method has 72239 packets. But the RSA and ROA have only 3840 packets and it reaches around 19.2 s and 4140 packets in 20.7 s for the same node 100. When the number of nodes is 160, the hybrid model has 229453.5 packets in 1202 s, where the single models have only 17357.4 in 93.3 s and 14928.9 packets in 78.1 s for the analysis of PND. Table 7 and Figure 2 show the experimental analysis of total number of live nodes for network 1.

When the initial rounds start, all the techniques have 100 nodes, but when the rounds are high, all techniques have different number of nodes. For instance, when the number of rounds is 1500, the RSA has 28 nodes and ROA has 30 nodes, but the proposed model has 90 nodes. This is due to the integration of RSA model and ROA model. When the number of rounds is 3500, the RSA has only 30 live nodes, ROA has 35 live nodes, and the proposed model has 91 live nodes. Finally, when the number of rounds is 5000, the proposed model has 82 live nodes, ROA has 35 live nodes, and RSA has 30 live nodes. Figure 3 presents the number of live nodes for proposed network 2.

In this second network, the initial nodes are 200 for zero rounds. When the number of rounds is increased, the live nodes for existing technique are less, when compared with the proposed model. When the number of rounds is 4500, the RSA has 125 nodes, ROA has 130 live nodes, and the proposed model has 187 live nodes. When the number of rounds is 2000, the proposed model has 183 live nodes, the RSA model has 130 nodes, and ROA has 138 live nodes. This

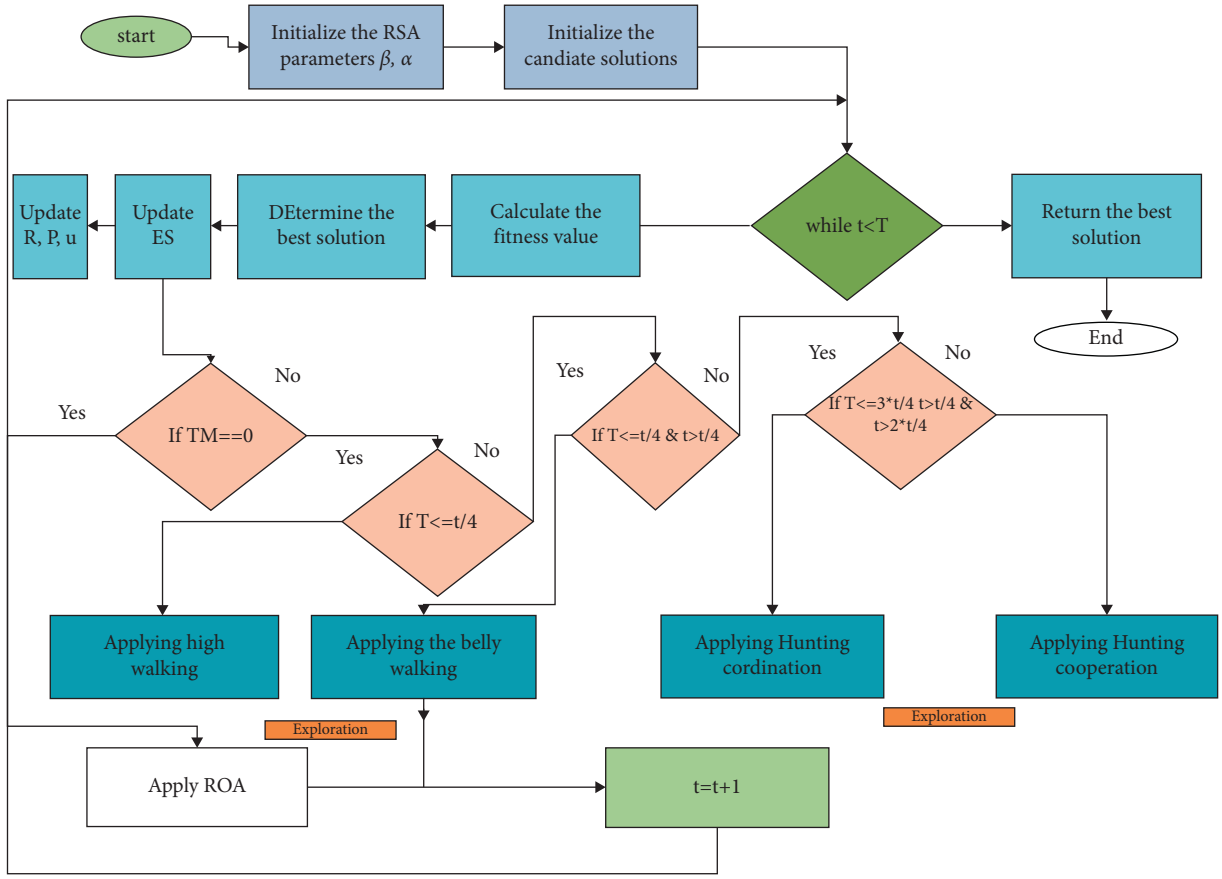

Figure 1: Flow chart of the proposed hybrid model.

(i) Initialize the TM parameter value ($TM = 0$).
(ii) sum$FF = 0$;
(iii) for ($t = 1$ to T)do
(iv) sumFF = sumFF + currentFF
(v) $C = (C + 1)$;
(vi) if (currentFF 6 = sumFF)then
(vii) if ($C > I$)then
(viii) TM = flip (TM);
(ix) sum$FF = 0$;
(x) $C = 0$;
(xi) end if
(xii) end if
(xiii) end for

Algorithm 1: The projected mean transition mechanism (MTM).

Table 3: Simulations scenario.

Network	Sink	Number of nodes	Area (m^2)
Proposed network 1	(0,0)	100	300 × 300
Proposed network 2	(250,250)	200	500 ×5 00

analysis shows that the number of lives nodes is higher for the proposed model compared to the existing techniques. Table 8 and Figure 4 show the remaining energy for network 1.

Initially, all models have 0.600 J, but when the number of nodes increases, the energy is also reduced. When the number of rounds is 500, the remaining energy of RSA is 0.111 J, that of ROA is 0.065 J, and that of the proposed model is 0.410 J. When the number of rounds is 2000, the remaining energy of RSA is 0.111 J, that of ROA is 0.055 J, and that of the proposed model is 0.340 J. When the number of rounds is 3500, the remaining energy of RSA is 0.111 J, that of ROA is 0.045 J, and that of the proposed model is 0.290 J. For the second network, the experimental values are shown in Table 9 and Figure 5.

When the number of rounds is 500, the proposed model has 0.360 J, ROA has 0.180 J, and RSA has 0.020 J. For all

Table 4: Parameters used in simulation.

Parameter	Value
$P_{DG\,\text{di spatch}}$	5 nJ/bit/message
P_{storage}	50 nJ/bit
P_{ESS}	10 pJ/bit/m2
$P_{DG\,\text{output}}$	0.0013 pJ/bit/m4
Packets size	8192 bits
Message size	100 bits
Energy of threshold down	0.01 J
Energy of threshold up	0.1 J

Table 5: Summary of FND and partial node death (PND) for proposed network 1.

Protocol	FND (100 nodes)		PND (90 nodes)		PND (80 nodes)	
	Time (s)	Packets	Time (s)	Packets	Time (s)	Packets
RSA	24.1	2410	53.2	5213.5	72.7	6901.2
ROA	40.1	3986.7	69.8	6535.6	95.5	8354.8
Hybrid RSA-ROA	44.4	40439	1288.6	125268.5	1150.8	12459

Table 6: Summary of FND and PND for proposed network 2.

Protocol	FND (200 nodes)		PND (180 nodes)		PND (160 nodes)	
	Time	Packets	Time	Packets	Time	Packets
RSA	19.2	3840	59.6	11584.3	93.3	17357.4
ROA	20.7	4140	50.4	9865.7	78.1	14928.9
Hybrid RSA-ROA	361.2	72239	868.5	170170	1202	229453.5

Table 7: Number of live nodes for proposed network 1.

Total no. of rounds	0	500	1000′	1500	2000	2500	3000	3500	4000	4500	5000
RSA	100	20	25	28	30	28	25	30	28	25	30
ROA	100	35	38	32	38	32	30	35	38	30	35
Hybrid RSA-ROA	100	90	88	90	83	87	90	91	90	87	82

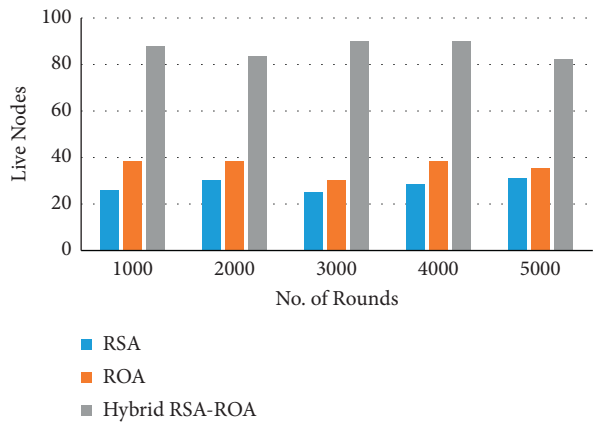

Figure 2: Graphical representation for network 1.

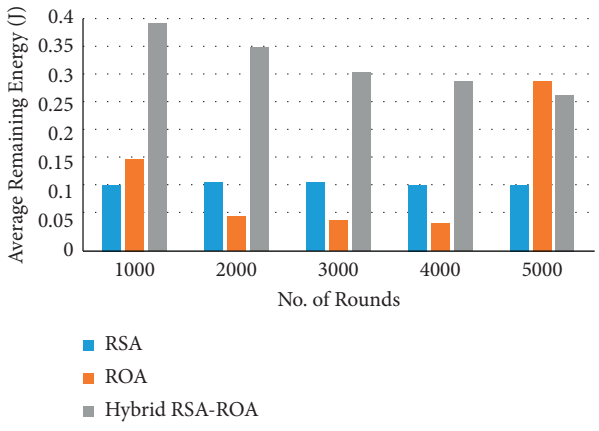

Figure 3: Graphical representation of the proposed model for energy.

different rounds, the existing RSA has stable remaining energy (i.e., 0.020 J). When the number of rounds is 1500, the proposed model has 0.200 J and ROA has 0.180 J. But, at one particular round, all techniques including the proposed model have stable remaining energy (i.e., 0.180 J). Table 10 shows the performance analysis of proposed model in terms of throughput.

The throughput of the proposed hybrid model is increased, when the number of nodes is also increased. In the throughput experiments for network 1, the RSA achieved 109 kbps, ROA achieved 114 kbps, and the proposed hybrid model achieved 157 kbps when the number of nodes reached 2000. These same techniques achieved 149 kbps, 170 kbps,

Table 8: Average remaining energy over different number of rounds for network 1.

Total no. of rounds	0	500	1000′	1500	2000	2500	3000	3500	4000	4500	5000
RSA	0.600	0.111	0.111	0.111	0.110	0.110	0.110	0.110	0.110	0.110	0.110
ROA	0.600	0.065	0.060	0.060	0.055	0.054	0.050	0.045	0.045	0.045	0.045
Hybrid RSA-ROA	0.600	0.410	0.380	0.360	0.340	0.32	0.300	0.290	0.280	0.270	0.260

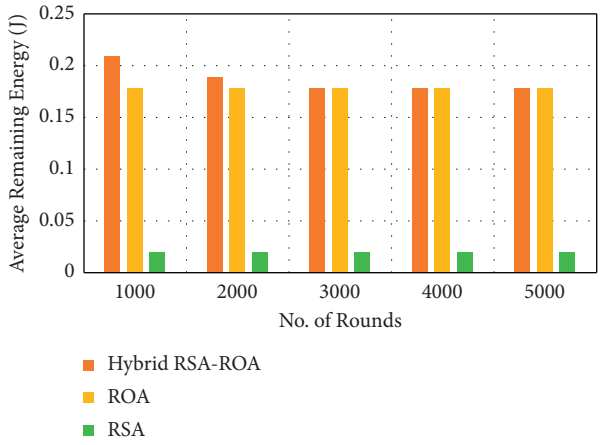

Figure 4: Graphical representation of the proposed model for remaining energy in network 2.

Table 9: Average remaining energy over different number of rounds for network 2.

Total no. of rounds	0	500	1000′	1500	2000	2500	3000	3500	4000	4500	5000
Hybrid RSA-ROA	0.60	0.360	0.210	0.200	0.190	0.180	0.180	0.180	**0.180**	0.180	0.180
ROA	0.60	0.180	0.180	0.180	0.180	0.180	0.180	0.180	0.180	0.180	0.180
RSA	0.60	0.020	0.020	0.020	0.020	0.020	0.020	0.020	0.020	0.020	0.020

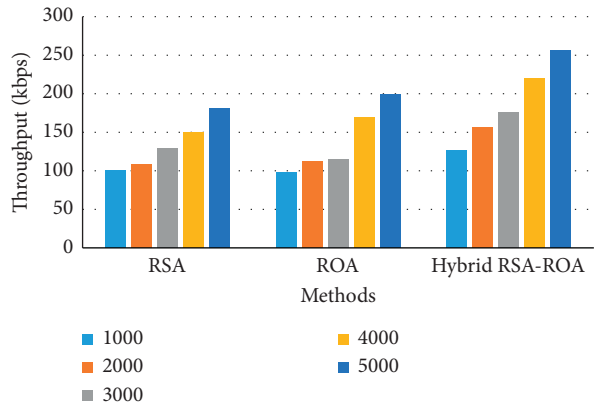

Figure 5: Graphical representation of the proposed method in terms of throughput for network 1.

and 220 kbps when the number of nodes reached 4000. Finally, when the number of nodes reached 5000, the RSA achieved 182 kbps, ROA achieved 200 kbps, and the proposed hybrid model achieved 255 kbps throughput. For proposed network 2, the RSA achieved 104 kbps, ROA achieved 119 kbps, and the proposed hybrid model achieved 136 kbps when the number of nodes reached 1000. These same techniques achieved 148 kbps, 159 kbps, and 189 kbps when the number of nodes reached 3000. Finally, when the number of nodes reached 5000, the RSA achieved 192 kbps, ROA achieved 220 kbps, and the proposed hybrid model achieved 263 kbps throughput. Figures 5 and 6 show the graphical analysis of the proposed hybrid model for both networks.

Table 11, Figure 7, and Figure 8show the experimental analysis of the proposed method for routing overhead for networks 1 and 2.

For proposed network 1, the routing overheads of RSA, ROA, and the hybrid model are 0.8, 0.7, and 0.5, respectively when the number of nodes is 2000. The RSA has 0.98, ROA has 0.9, and the proposed hybrid model consumed only 0.82 routing overhead when the number of nodes reached 4000. From this analysis, it is clearly proven that

Table 10: Validated analysis of the proposed method for throughput (kbps).

No. of nodes	Proposed network 1			Proposed network 2		
	RSA	ROA	Hybrid RSA-ROA	RSA	ROA	Hybrid RSA-ROA
1000	100	98	126	104	119	136
2000	109	114	157	120	128	166
3000	128	115	176	148	159	189
4000	149	170	220	159	190	234
5000	182	200	255	192	220	263

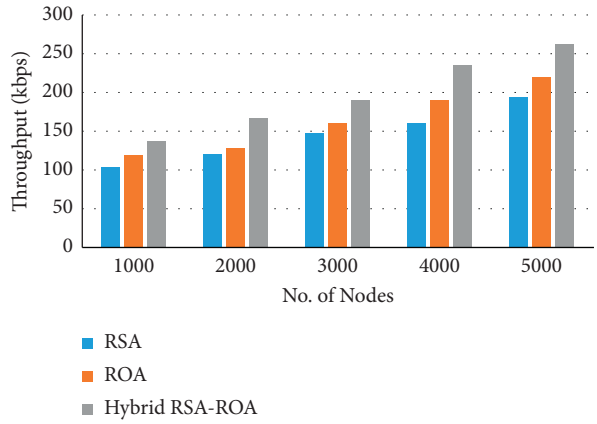

Figure 6: Graphical representation of the proposed method in terms of throughput for network 2.

Table 11: Performance analysis of the proposed method for routing overhead.

No. of nodes	Proposed network 1			Proposed network 2		
	RSA	ROA	Hybrid RSA-ROA	RSA	ROA	Hybrid RSA-ROA
1000	0.7	0.6	0.4	0.63	0.51	0.49
2000	0.8	0.7	0.5	0.70	0.58	0.46
3000	0.9	0.7	0.62	0.69	0.63	0.57
4000	0.98	0.9	0.82	0.71	0.69	0.74
5000	1.23	1.18	0.96	1.26	1.07	0.82

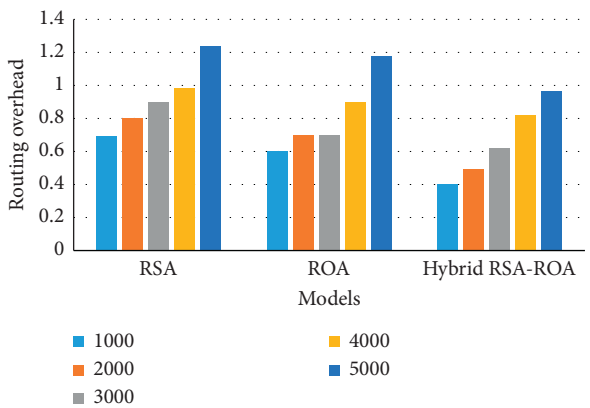

Figure 7: Graphical representation of the proposed method in terms of routing overhead for network 1.

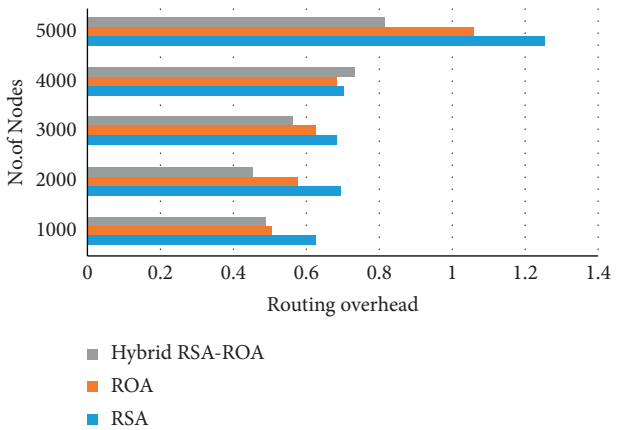

Figure 8: Graphical representation of the proposed method in terms of routing overhead for network 2.

the number of nodes influences the performance of routing overhead of each model. The hybrid model achieved 0.49 to 0.82 of routing overhead when the numbers of nodes were 1000 to 5000, while the single models, RSA and ROA, achieved 0.63 to 1.26 and 0.51 to 1.07 of routing overhead when numbers of nodes were 1000 to 5000. Figure 8 shows the graphical analysis of proposed network 2 in terms of routing overhead.

5. Conclusion

In this paper, the optimum generation programming was studied using the hybrid model in the power system. The proposed method was implemented keeping in mind maximum renewable energy harvest and minimization of energy losses. The optimal solutions for the proposed method were identified and obtained by integrating RSA and ROA algorithms. The comparative cases of single technique with hybrid model were made to exploit the potential and effectiveness of the proposed method in two different networks, where the single models, RSA and ROA, achieved 0.63 to 1.26 and 0.51 to 1.07 of routing overhead, respectively, when the numbers of nodes were 1000 to 5000. The simulation results showed the effectiveness and good performance of the proposed method for obtaining optimal solutions for generation programming, especially with maximum harvesting of renewable energy and minimizing energy losses. Energy losses were clearly low depending on the optimum storage power of the ESS and minimizing line losses with maximum renewable energy harvest. In addition, the maximum renewable energy harvest is greatly affected by the reduction of conventional generations and reduced ESS losses.

Data Availability

No data were used to support the findings of this study.

Conflicts of Interest

The authors declare that they have no conflicts of interest.

References

[1] D. Praveen Kumar, A. Tarachand, and A. C. S. Rao, "Machine learning algorithms for wireless sensor networks: a survey," *Information Fusion*, vol. 49, pp. 1–25, 2019.

[2] D. Praveen Kumar, A. Tarachand, and A. C. S. Rao, "ACO-based mobile sink path determination for wireless sensor networks under non-uniform data constraints," *Applied Soft Computing*, vol. 69, pp. 528–540, 2018.

[3] J. Yick, B. Mukherjee, and D. Ghosal, "Wireless sensor network survey," *Computer Networks*, vol. 52, no. 12, pp. 2292–2330, 2008.

[4] I. F. Akyildiz, W. Su, Y. Sankarasubramaniam, and E. Cayirci, "Wireless sensor networks: a survey," *Computer Networks*, vol. 38, no. 4, pp. 393–422, 2002.

[5] F. K. Shaikh and S. Zeadally, "Energy harvesting in wireless sensor networks: a comprehensive review," *Renewable and Sustainable Energy Reviews*, vol. 55, pp. 1041–1054, 2016.

[6] A. A. Babayo, M. H. Anisi, and I. Ali, "A review on energy management schemes in energy harvesting wireless sensor networks," *Renewable and Sustainable Energy Reviews*, vol. 76, pp. 1176–1184, 2017.

[7] H. Yu and Q. Yue, "Indoor light energy harvesting system for energy-aware wireless sensor node," *Energy Procedia*, vol. 16, pp. 1027–1032, 2012.

[8] D. Daniel, N. Preethi, A. Jakka, and S. Eswaran, "Collaborative intrusion detection system in cognitive smart city network (CSC-net)," *International Journal of Knowledge and Systems Science*, vol. 12, no. 1, pp. 60–73, 2021.

[9] F. Akhtar and M. H. Rehmani, "Energy replenishment using renewable and traditional energy resources for sustainable wireless sensor networks: a review," *Renewable and Sustainable Energy Reviews*, vol. 45, pp. 769–784, 2015.

[10] A. Cammarano, C. Petrioli, and D. Spenza, "Online energy harvesting prediction in environmentally powered wireless sensor networks," *IEEE Sensors Journal*, vol. 16, no. 17, pp. 6793–6804, 2016.

[11] H. Cheng, Z. Su, N. Xiong, and Y. Xiao, "Energy-efficient node scheduling algorithms for wireless sensor networks using Markov random field model," *Information Sciences*, vol. 329, pp. 461–477, 2016.

[12] D. A. Guimaraes, E. P. Frigieri, and L. J. Sakai, "Influence of node mobility, ˜ recharge, and path loss on the optimized lifetime of wireless rechargeable sensor networks," *Ad Hoc Networks*, vol. 97, Article ID 102025, 2020.

[13] A. Shawahna, M. E. Haque, and M. E. Tozal, "Energy harvesting in wireless sensor network with efficient landmark selection using mobile actuator," in *Proceedings of the: 2017 Annual IEEE International Systems Conference (SysCon)*, pp. 1–8, IEEE, Montreal, QC, Canada, April 2017.

[14] S. Sakya, "Design of hybrid energy management system for wireless sensor networks in remote areas," *Journal of Electrical Engineering and Automation (EEA)*, vol. 02, pp. 13–24, 2020.

[15] F. K. Shaikh and S. Zeadally, "Energy harvesting in wireless sensor networks: a comprehensive review," *Renewable and Sustainable Energy Reviews*, vol. 55, pp. 1041–1054, 2016.

[16] S. Kim, R. Vyas, J. Bito et al., "Ambient RF energy-harvesting technologies for self-sustainable standalone wireless sensor platforms," *Proceedings of the IEEE*, vol. 102, no. 11, pp. 1649–1666, 2014.

[17] H. Sharma, A. Haque, and Z. A. Jaffery, "Maximization of wireless sensor network lifetime using solar energy harvesting for smart agriculture monitoring," *Ad Hoc Networks*, vol. 94, Article ID 101966, 2019.

[18] R. S. Liu and Y. C. Chen, "Robust data collection for energy-harvesting wireless sensor networks," *Computer Networks*, vol. 167, Article ID 107025, 2020.

[19] V. Gupta and S. De, "Collaborative multi-sensing in energy harvesting wireless sensor networks," *IEEE Transactions on Signal and Information Processing over Networks*, vol. 6, pp. 426–441, 2020.

[20] D. K. Sah and T. Amgoth, "A novel efficient clustering protocol for energy harvesting in wireless sensor networks," *Wireless Networks*, vol. 26, no. 6, pp. 4723–4737, 2020.

[21] N. Qi, Y. Yin, K. Dai, C. Wu, X. Wang, and Z. You, "Comprehensive optimized hybrid energy storage system for long-life solar-powered wireless sensor network nodes," *Applied Energy*, vol. 290, Article ID 116780, 2021.

[22] S. Mohsen, A. Zekry, K. Youssef, and M. Abouelatta, "A self-powered wearable wireless sensor system powered by a hybrid energy harvester for healthcare applications," *Wireless Personal Communications*, vol. 116, no. 4, pp. 3143–3164, 2021.

[23] J. Wu, M. Xu, F. F. Liu, M. Huang, L. Ma, and Z. M. Lu, "Solar wireless sensor network routing algorithm based on multi-objective particle swarm optimization," *J. Inf. Hiding Multim. Signal Process.*vol. 12, no. 1, pp. 1–11, 2021.

[24] K. Panagiotou, C. Klumpner, and M. Sumner, *The Effect of Including Power Converter Losses when Modelling Energy Storage Systems: A UK Domestic Study*, EPE'16 ECCE Europe, Europe, 2016.
[25] J. Grainger and W. Stevenson, *Power System Analysis*, McGraw-Hill, New York, Ny, USA, 1994.
[26] L. Abualigah, M. Abd Elaziz, P. Sumari, Z. W. Geem, and A. H. Gandomi, "Reptile Search Algorithm (RSA): a nature-inspired meta-heuristic optimizer," *Expert Systems with Applications*, vol. 191, Article ID 116158, 2022.
[27] H. Jia, X. Peng, and C. Lang, "Remora optimization algorithm," *Expert Systems with Applications*, vol. 185, Article ID 115665, 2021.